First millimeter mapping of the jet and nucleus of M 87

Vincent Despringre, Didier Fraix-Burnet, Emmanuel Davoust

Astron. Astrophys. 309, 375–380 (1996)

ASTRONOMY AND ASTROPHYSICS

First millimeter mapping of the jet and nucleus of M 87

V. Despringre, D. Fraix-Burnet*, and E. Davoust

Laboratoire d'Astrophysique, Observatoire Midi-Pyrénées, 14 Avenue Edouard Belin, F-31400 Toulouse, France
e-mail: despring@obs-mip.fr

Received 27 July 1995 / Accepted 5 September 1995

Abstract. Observations of M 87 at 89 GHz (3.4 mm) with the IRAM Plateau de Bure interferometer are presented. This is the first image of an extragalactic jet at this frequency with such a resolution ($2\farcs9 \times 1\farcs8$). Knots A, B, C and G in the jet are clearly seen. The photometry of the knots reveals that, within the error bars, the millimetric intensity is that expected from a linear interpolation between the radio and optical values. An extended feature of about $13'' \times 7''$ appears around the nucleus, which we were not able to attribute to an artifact. It is elongated perpendicular to the jet and its offcentering from the nucleus is symmetric to that of the well known H_α emission-line features in M 87. If interpreted as very cold gas ($T \lesssim 10$ K), this extended structure would then have a total mass of $\simeq 10^{12}$ $M_\odot$.

Key words: galaxies: individual: M 87 – galaxies: jets – radio continuum: galaxies – galaxies: ISM

1. Introduction

The jet of M 87 was the first discovered extragalactic jet (Curtis 1918), and as the closest to us, is one of the best studied cases. A few hundred are now known at radio wavelengths, while only a few have been found in the optical: M 87, 3C273, 3C66B, PKS0521-36, 3C264 (Crane et al. 1993), 3C120 (Lelièvre et al. 1994) and possibly 3C449 (Capetti et al. 1994) and Cen A (Brodie & Bowyer 1985). The spectrum of extragalactic jets corresponds to pure synchrotron emission; it is a power law with a cutoff frequency well seen in the optical jets (Meisenheimer & Heavens 1986, Fraix-Burnet & Nieto 1988, Fraix-Burnet et al. 1991). However in the case of M 87, X-ray emission from the two brightest knots indicates that this cutoff frequency could be in the X-rays (Biretta et al. 1991). An intriguing question is why there are so few jets seen at optical wavelengths, or equivalently, why the cutoff frequency is generally not in the optical, but rather in the infrared or even in the sub- millimeter domain (Fraix-Burnet et al. 1991). The answer is undoubtedly related to the efficiency of the acceleration of the relativistic electrons responsible for the synchrotron emission (Fraix-Burnet & Pelletier 1991). Whereas the presence of some optical jets is a very stringent requirement for the acceleration models, it would be of great importance to know more precisely where the cutoff frequency of the non-optical jets is located. The presence of a break at low frequency somewhere in the synchrotron spectrum is another feature that constrains the model parameters, but its precise location is unknown for most jets, because of the lack of photometry in the millimeter domain.

Biretta et al. (1991) compiled the information available at all wavelengths at a resolution of about $2''$ on the jet of M 87 and clearly showed that the observations in the radio and in the optical are compatible with a single power law. Meisenheimer & Heavens (1986) went a step further on the jet of 3C273 by fitting a synchrotron spectrum model to the spectrum of the hot-spot. However, the interpolation range in frequency is so large that some freedom in the parameters is allowed and, furthermore, one cannot exclude that the optical emission of jets has a different spectrum from that seen in the radio. More recently, Meisenheimer et al. (1995) performed the same kind of fit for the integrated emission of knots A, B, and C in the M 87 jet.

It was thus necessary to fill the gap between radio and optical wavelengths in the synchrotron spectrum of optical jets. The required observation had to be of high sensitivity and high spatial resolution (of the order of $1''$).

IRAS data are available but are of little interest for the spectrum of individual knots. In the millimeter domain, new and very sensitive instruments are now operational. Salter et al. (1989) certainly detected the jet of M 87 at 230 GHz with the IRAM 30 m telescope on Pico Veleta. However the resolution ($11''$) prevents a definite localization of the millimeter radiation in the jet itself and is insufficient for obtaining the spectra of the individual knots.

The above remarks also hold for the nucleus of M 87 which has to be well distinguishable from the huge radio lobe to provide a reliable spectrum. The IRAM Plateau de Bure interferometer is well suited for this purpose because of its high sensitivity and resolution.

Send offprint requests to: V. Despringre

* *Present address:* Laboratoire d'Astrophysique de Grenoble, BP 53X, F-38041 Grenoble Cédex, France

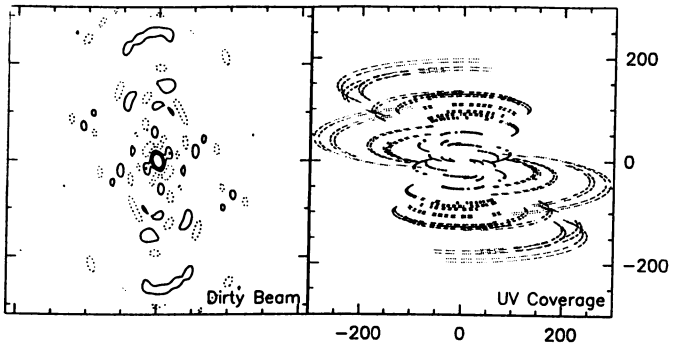

Fig. 1. Dirty beam (size of field: 64″×64″) and uv-coverage (in metre units) of the whole set of observations.

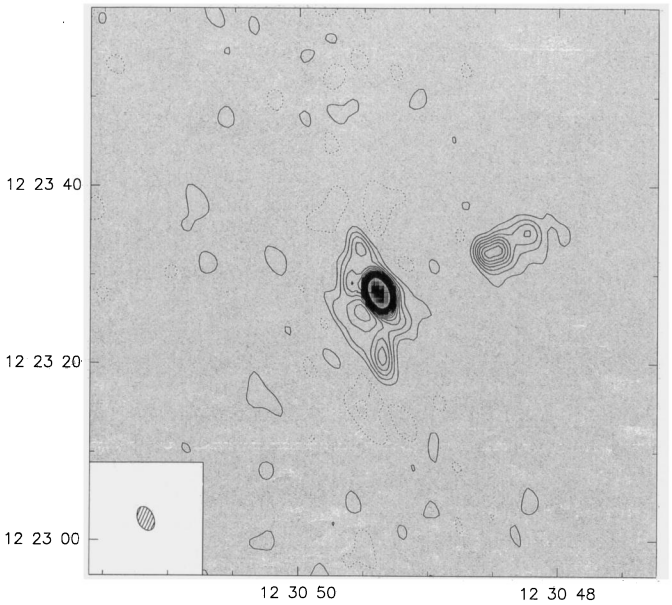

Fig. 2. Grey map of M 87 with contour level spacing of 35 mJy/beam and a peak intensity of 1.67 Jy/beam. The beamwidth is 2.″9 × 1.″8 at PA=22°.

Another reason for observing M 87 at millimeter wavelengths is that molecular lines and thermal emission from cold dust are detectable in this range. M 87 is known for having little molecular gas, since no CO (of total mass ¡10^7 $M_\odot$ within 2 kpc) and no HI have been found (Braine & Wiklind, 1993). However, as pointed out by Daines et al. (1994), the emission lines from clouds close to the nucleus would be broad, making their detection quite difficult. They suggest that the cooling flow in M 87 could form cold dust-free clouds of primarily atomic gas. These clouds would present broad HI emission lines, hence difficult to detect, but also a thermal emission with $T \lesssim 10$K, which could be detected in the millimeter range.

2. Observations and data reduction

The observations were made at the IRAM Plateau de Bure interferometer (Guilloteau et al. 1992) with three antennas between November 1992 and January 1993 with the BC set of configurations. For some unknown reason, the most compact configuration on November 2, 1992, showed strange behavior in phase and amplitude and was thus not used. Complementary observations with four antennas were made in the two compact configurations C2 and D in March, 1994. The central frequency of the observations was 88.26 GHz, in order to optimize atmospheric conditions at Plateau de Bure and to enable us to search for HCN (J=1→0) at 88.63 GHz as a byproduct. The spectral resolution of the correlator was set to 2.5 MHz for a total bandwidth of 500 MHz. The data reduction was performed with GILDAS. The total uv-coverage and the dirty beam are presented in Fig. 1. The pixel size was set to 0.″5 and the dirty map was then CLEANed.

Three calibrators (3C84, 3C273 and 1308+326) were used for the three antenna observations and two (3C273 and 3C279) for the four antenna runs. The 3C273 source has a jet of similar angular size as that of M 87, but mapping this quasar after calibration on 3C279 of the four antenna data did not reveal any hints for the jet. Any contamination by the jet of 3C273 is thus extremely improbable. The intensity of 3C273 was 21.5 Jy during the three antenna observations, and 22.2 Jy during the four antenna observations. The intensity of the center of M 87 was assumed to be constant, even though it is variable at 90 GHz with an amplitude of about 1 Jy over a year (Steppe et al. 1988). In principle, intensity variations of the nucleus between the different configurations could lead to artifacts when mapping with the whole set of data. Essentially, the shape of the variable object is affected. However, in our case where the variable source is unresolved, it is rather easy to detect such artifacts by comparing maps obtained with configurations taken individually. Down to the noise level, the shape of the nucleus is consistent from one configuration to the other, and the extended structures of the field are detected on all maps (of course more clearly with shorter baselines). The photometry of the nucleus derived from our data is thus a sort of average of the intensity of the nucleus during this 18-month period. But since the jet is not significantly variable (Biretta et al. 1989), its photometry is certainly not very much affected by this problem.

The photometry was performed in three ways. The first uses the task UV_FIT in GILDAS and fits a point source (for the nucleus and knot C) or an elliptical gaussian (for knots A and B together) directly from the visibilities. The two other methods make use of the IRAF package. One is simply an integration within boxes as close as possible to those used by Biretta et al. (1991), and the other is an integration along the profile of the jet (Sect. 3.2). The profile of the jet is obtained in a 5″ wide slit along the jet with a step of 0.″5.

The measured intensities are of course affected by the variability of the nucleus of M 87 as well as that of the calibrators. The corresponding error is difficult to assess, but it might be as high as a few tenths of Jy. The jet being highly polarized (up to 20% at this resolution; see Fraix-Burnet et al. 1989), the measured intensities depend on the relative position of the polarization vectors of the object and of the receptor, an angle that varies in time during the observations and from knot to knot. In the case of knots A and B, of similar polarization (about 20%)

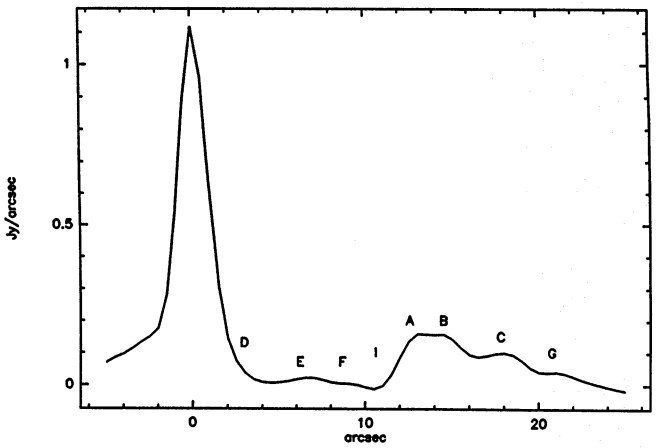

Fig. 3. Profile along the jet obtained in a 5″ wide slit with a step of 0.″5.

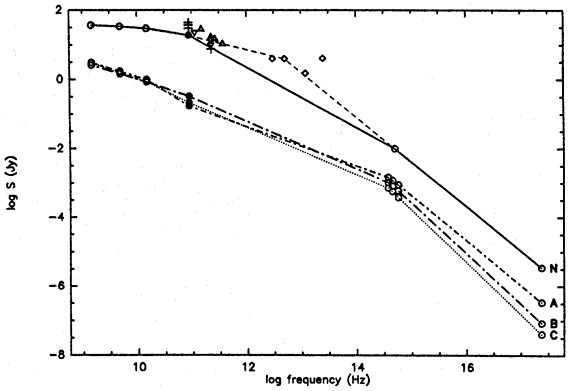

Fig. 4. Spectra of the nucleus and knots of the jet. All values for the nucleus have been multiplied by 10 for clarity of the plot. Straight lines connect individual data points for a given feature. Knot A: dash–dot line; knot B: long dash–dot line; knot C: dotted line. For the nucleus, the solid line connects high resolution measurements while the dashed line includes the 5000 GHz (60 μm) IRAS point as well. The black dots (•) are from the present work and open circles (○) are values taken from Biretta et al. (1991). Low resolution values are from +: Steppe et al. (1988); ▽: Braine & Wiklind (1993); △: Knapp & Patten (1991); □: Salter et al. (1989); ◇: Young et al. (1989).

but with different position angles (Fraix-Burnet et al. 1989), the relative intensity between the two knots can be biased by a factor of 1.5 at most. All these uncertainties are not taken into account in the following, where error bars only refer to the error on the measure itself.

3. Results

The final map of M 87 at 89 GHz after CLEANing is shown in Fig. 2. The beam is 2.″9 × 1.″8 (PA=22°). We discuss separately the three features that are conspicuous on the map: the nucleus, the jet and the extended structure around the nucleus. An upper limit on the content of HCN is given is Sect. 3.4.

3.1. The nucleus of M 87

It is clear that, in our data, the nucleus is embedded in an extended structure that will be discussed in Sect. 3.3. The UV_FIT task, which is able to separate the two components (see Sect. 2), gives 1.88 ± 0.1 Jy for the intensity of the nucleus of M 87 at 89 GHz. The overall spectrum is discussed in Sect. 4.1.

3.2. The jet

The jet with knots A, B, C and G, is clearly seen. Knots D, E, F, and I, located between the nucleus and knot A, are not detected. The lobes are invisible, certainly because of a lack of dynamic range with the compact configurations which have only four antennas. No hint for any detectable emission is present on the counterjet side.

The profile along the jet (Fig. 3) shows knots A, B, C, and G quite well. Some "humps" seem to be present at the location of knots E and F, but this is certainly not significant. The resolution is not sufficient to individualize knots D and I, which could not have been seen anyway because of their low brightness (assuming the same relative intensity between knots as at cm wavelengths).

Measuring the intensity of the knots in the same rectangular areas as those used by Biretta et al. (1991) for knots A (box size = 2.″0×4.″5), B (3.″0×4.″5), and C (3.″0×4.″5) gives respectively: 0.17 ± 0.03, 0.33 ± 0.06 and 0.22 ± 0.04 Jy. The relative intensities of knots A and B are of course very uncertain because the choice of the boxes is quite arbitrary. An interesting comparison can be made with the results from task UV_FIT which gives an intensity of 0.58 Jy for knots A and B together (as compared with 0.50 Jy above) and 0.13 Jy for knot C. The integrated intensity for these three knots is then about 0.72 Jy for both methods. The total intensity of the jet measured on the profile from knot I outward is 1.0 Jy, and it is 1.14 Jy when measured in a large area comprising the inner (invisible) part of the jet.

3.3. The extended feature around the nucleus

A rather strong extended feature is clearly seen around the nucleus. Since such a component has never been noticed before at any wavelength, we thoroughly looked for an instrumental or deconvolution effect. We rejected a possible line emission region (from HCN), after examining separately the lower and upper sideband maps which turn out to be identical. Calibration, baseline, weather or receiver problems were eliminated, notably because the feature appears on all maps made with individual configurations. It is more conspicuous on compact configurations (mainly four antenna observations), indicating that the feature is extended with no detailed structure in it. As mentioned in Sect. 2, this is also against an artifact caused by the variability of M 87. Using 3C279 as the calibrator for the

four antenna data on M 87 yields the same result, and mapping 3C279 with 3C273 as the calibrator yields a point source with no strange artifacts. Also, the feature does not correspond to any structure in the dirty beam, even though the two Northern and Southern peaks are close to similar features on the dirty beam. Moreover, we tried to remove the nucleus (using the UV_FIT task; see Sect. 2) before CLEANing. We also used a new deconvolution technique, called WIPE (Lannes et al. 1994, 1995), which uses a totally different approach than CLEAN. In both cases, the feature is still present with exactly the same structure, showing that this is not an artifact of the deconvolution. A better test would have been to self-calibrate the data but this is practically not feasible with only four antennas.

The structure is essentially elongated ($12''.7 \times 6''.5$) perpendicular to the jet. It is not centered on the nucleus; the offset is about $1''.5$ to the SE. There are 4 peaks, the maximum brightness being 0.2 Jy/beam, and a "hole" at the center of the structure. The total intensity (after removal of the nucleus) is 1.4 Jy. Note that the whole structure seems to be symmetric with respect to its center. This property could be in favor of an artifact.

At this stage, we must conclude that either it is an important artifact caused for a subtle reason not understood at this time, or this feature is real. Some astrophysical arguments, discussed in Sect. 4.3, lead us to believe that this structure could be real.

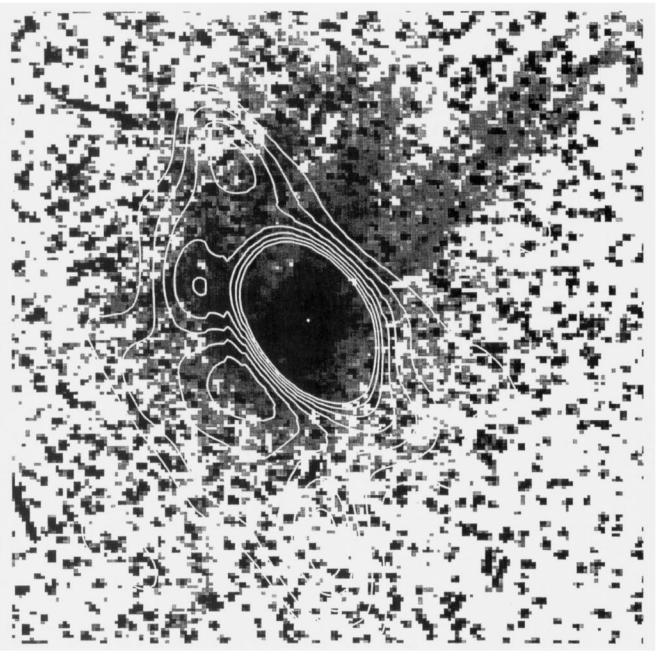

Fig. 5. Contour of Fig. 2 clipped at 0.25 Jy/beam and overlaid on an Hα+[NII] picture from HST.

3.4. HCN

As already mentioned in Sect. 3.3, no HCN emission is detected. This provides an upper limit of $\simeq$ 0.03 Jy/beam over a 160 MHz bandwidth for a 2.5 MHz spectral resolution.

4. Discussion

4.1. The nucleus

Limiting ourselves to data with resolution of about 2–3″ (solid line in Fig. 4), that is data compiled by Biretta et al. (1991) plus our value at 89 GHz, we find a steepening of the spectrum occurring at about 50 GHz. This indicates that the break frequency is around 100–1000 GHz. No fit with a synchrotron spectrum is attempted here, but it can be easily guessed that such a spectrum would lie between the solid and the dashed lines in Fig. 4 (see Meisenheimer & Heavens 1986, and Meisenheimer et al. 1995, for examples of such a fit).

However, in this picture, the IRAS data at 25000, 12000, 5000 and 3000 GHz (respectively 12 , 25, 60 and 100 μm; Young et al. 1989) are slightly higher than the above synchrotron spectrum. This could be explained by the low resolution of IRAS observations that probably include other components than the nucleus alone (for instance, Young et al., 1989, suggest that the 12 μm point is biased by cool stars). The interpretation of the spectrum of the nucleus of M 87 is complicated by its variability which, in the mm domain, is obvious on Fig. 4. Steppe et al. (1988) found that M 87 is variable by about 1 Jy/year at 90 GHz. Nevertheless, the low-resolution measurements between 90 and 150 GHz are all higher than the synchrotron spectrum guessed from high resolution data. We believe that this could be the signature of the extended feature discussed in Sect. 4.3. Low resolution data between 230 and 375 GHz are consistent with the synchrotron spectrum.

The conclusion is that the high resolution spectrum of the nucleus is consistent with a single power law synchrotron spectrum with a break frequency between about 10^{11} and 10^{12} GHz. Low resolution observations seem to reveal the presence of a slight excess at $\simeq$ 100 GHz.

4.2. The jet

The structure of the jet is unsurprisingly similar to what is known at other wavelengths. More interesting are the spectra of knots A, B and C (Fig. 4). Within the error bars, our mm values fit the linear interpolation between cm and optical wavelengths. Our point for knot A seems to be a little bit too low. Knot A is also less prominent on the profile (with respect to knot B; Fig. 3) than at other wavelengths. No significant negative feature is present on the dirty beam at this position, and no gap deeper than -0.03 Jy/arcsec is seen anywhere on similar profiles made on the opposite side of the jet as well as North and South of it. The apparently low value for knot A is then probably explained by the choice of the box for the intensity measurement, together with a polarization effect (see Sect. 2).

As noted by Biretta et al. (1991), the difference between the spectral indices in the radio cm ($\alpha_{rr} \simeq 0.5$) and in the optical ($\alpha_{oo} \simeq 1.3$) domains implies a break in-between. Our data lie on the linear interpolation between cm and optical wavelengths ($\alpha_{ro} \simeq 0.6$), showing that a gentle break does occur at mm wavelengths. We conclude that two breaks could be present: one at around 1 GHz, where no observation of individual knots is available yet, and one at about 3 10^{14} Hz, i.e. in the opti-

cal. The optical break cannot be the break frequency where the synchrotron losses become a significant fraction of the energy of the electrons. Since this break frequency is inversely proportional to the third power of the magnetic field (Heavens & Meisenheimer, 1987), this would mean a very low magnetic field ($\lesssim 10^{-2}$ nT), well below the typical equipartition value (10 to 100 nT). A more reasonable alternative is that the true break frequency is below 1 GHz and the optical break is indeed the cutoff frequency. The interpretation of the X-ray emission in this context probably requires the introduction of several electron populations and/or inhomogeneous jet models (see discussions in Biretta et al. 1991 and Meisenheimer et al. 1995).

4.3. The extended feature around the nucleus

We were not able to explain away the feature described in Sect. 3.3 as an artifact, so let us then analyze if it is astrophysically plausible.

It is elongated perpendicular to the jet and lies in the same region (radius between 3 and 8″) where Sparks et al. (1988) found the optical isophotes of the galaxy to be perpendicular to the jet. Zeilinger et al. (1993) establish that this orientation actually depends on the color band, indicating the possible presence of dust. However, dust absorption at optical wavelengths have been noticed only along the emission line filaments (Ford et al., 1994). On Fig. 5, the contours of our 89 GHz data are overlaid onto a Hubble Space Telescope Hα+N[II] image. This image was obtained by subtracting a broad band image (average of two F507M images) to the average of two narrow band (F658N) images. The individual frames were retrieved from the HST archives. These data are discussed in Ford et al. (1994). There is a huge difference in resolution between the mm and the optical image, but i) the orientation of the elongated structure is only about 20° from the 1″ disklike structure with spiral arms described in Ford et al. (1994), ii) its NW part is flat and perpendicular to the emission line filaments, and iii) it is offset from the nucleus toward the opposite side of the ionized filaments. The position and shape of the extended feature are thus not unrelated to other characteristics of the M 87 galaxy.

No counterpart is present at cm wavelengths (see for example Owen et al. 1990), and the resolution ($> 11''$) of the maps at higher wavelengths is insufficient for allowing the detection of any such structure. However, using the integrated flux with the known synchrotron contribution from the nucleus, one can hope to constrain its spectrum with intensity measurements between 90 and 5000 GHz. As noticed in Sect. 4.1, there seems to be a slight excess in the nucleus spectrum at $\simeq$ 100 GHz (see Fig. 4). Coadding our values for the intensities of the nucleus and of the extended feature (i.e. 3.3 Jy), we find that it is consistent with the measures (between 2.98 and 4.39 Jy) by Steppe et al. (1988) at 90 GHz at several epochs. This is in favor of the reality of the extended feature and shows that its spectrum is rather narrowly peaked at $\simeq$ 100 GHz.

Clearly, thermal radiation from very cold dust at $T \lesssim 10$ K could explain the properties of this component. Estimating the dust mass from the total intensity as in McMahon et al. (1994) and for a distance to M 87 of 15 Mpc, one obtains: $M_{\rm dust} \simeq 4\ 10^{12}\ M_\odot$. This is an enormous amount of dust, within a region of about 1 kpc×0.5 kpc. Assuming the extinction in M 87 to be similar to that in our Galaxy, Goudfrooij et al. (1994) find $10^3\ M_\odot$ of dust in M 87. This mass would be higher for smaller grain sizes. For elliptical galaxies with dust lanes, they find typically 10^6–$10^7\ M_\odot$ of dust, but M 87 should be closer in its properties to Radio Quiet Quasar in which Hughes et al. (1993) find 10^8–$10^9\ M_\odot$ of dust. Our value of $\simeq 4\ 10^{12}\ M_\odot$ compares roughly with the total amount of gas accreted by a cooling flow during 10 Gyr with a rate of more than 10 $M_\odot$/yr (White & Sarazin, 1988), with the total amount ($10^{12}\ M_\odot$) of hot gas in the halo of M 87 as estimated by Binney & Cowie (1981), and also with the total mass ($6\ 10^{12}\ M_\odot$) within 50 kpc as derived by Merritt & Tremblay (1993). Because neither CO nor HI have been detected in M 87 (Braine & Wiklind 1993), our data could find an explanation in the work by Daines et al. (1994): it could be dust-free, primarily atomic, clouds with $T \lesssim 10$ K which are the sink of the cooling flow. Very little CO would be present and the HI line would be too broad for easy detection.

On astrophysical grounds, it is thus plausible that the extended feature we detect around the nucleus of M 87 is real.

5. Conclusion

The present work demonstrates that interferometry at millimeter wavelengths brings invaluable information to the investigation of extragalactic radio sources. In the case of jets, the shape of the synchrotron spectrum is important for understanding the physical conditions leading to the radiation. For M 87, it appears that the break frequency must be near 1 GHz and that another break, probably the cutoff, occurs at optical wavelengths. A unique synchrotron spectrum from a homogeneous medium would certainly be difficult to fit to the data from the radio to the X-rays. But recent high resolution observations with the VLA or the HST reveal that the jet is far from homogeneous, being rather filamentary. This kind of study will have to be done for non-optical jets to pinpoint, not only the break frequency, but also the position of the cutoff frequency which is in the submillimeter or far- infrared region.

Millimeter wavelengths are also the realm of dust and molecules. The link between the radio emission from the jets and lobes and the dust component of the ISM could explain the different shapes of radiosources. The monster at the center of radiogalaxies must be fed somehow by accretion of matter. Millimeter mapping of dust and molecules at high resolution could tell us where this matter comes from, and thus why most galaxies and quasars are radio-quiet. In this paper, we find an extended feature around the nucleus of M 87. While it is difficult to entirely eliminate observational or instrumental artifacts, there are some arguments in favor of its reality. The most reasonable astrophysical interpretation points to a huge cloud of very cold atomic gas. No such thing has ever been observed in other galaxies simply because this is the first mapping of an extragalactic object with this resolution and sensitivity. Complementary observations are considered to confirm this result.

Acknowledgements. We would like to thank Stéphane Guilloteau for invaluable advice and help covering all aspects of the observations and data reduction with the Plateau de Bure interferometer. Discussions with Alain Baudry, Nathalie Brouillet and Didier Despois helped us in defining this project. The referee, Klaus Meisenheimer, is thanked for his prompt interesting remarks for improving the paper.

References

Binney J., Cowie L.L., 1981, ApJ 247, 464
Biretta J.A., Owen F.N., Cornwell T.J., 1989, ApJ 342, 128
Biretta J.A., Stern C.P., Harris D.E., 1991, AJ 101, 1632
Braine J., Wiklind T., 1993, A&A 267, L47
Brodie J., Bowyer S., 1985, ApJ 292, 447
Capetti A., Macchetto F., Sparks W.B., Miley G.K., 1994, A&A 289, 61
Crane et al., 1993, ApJ 402, L37
Curtis H.D., 1918, Publ. of Lick Observatory 13, 31
Daines S.J., Fabian A.C., Thomas P.A., 1994, MNRAS 268,1060
Ford H.C., Harms R.J., Tsvetanov Z.I. et al., 1994, ApJ 435, L27
Fraix-Burnet D., Golombek D., Macchetto F.D., 1991, AJ 102, 562
Fraix-Burnet D., Le Borgne J.-F., Nieto J.-L., 1989, A&A 224, 17
Fraix-Burnet D., Nieto J.-L., 1988, A&A 198, 87
Fraix-Burnet D., Pelletier G., 1991, ApJ 367, 86
Goudfrooij P., de Jong T., Hansen L., Nørgaard-Nielsen H.U., 1994, MNRAS 271, 833
Guilloteau S., Delannoy J., Downes D. et al., 1992, A&A 262, 624
Heavens A.F., Meisenheimer K., 1987, MNRAS 225, 335
Hughes D.H., Robson E.I., Dunlop J.S., Gear W.K., 1993, MNRAS 263, 607
Knapp G.R., Patten B.M., 1991, AJ 101, 1609
Lannes A., Anterrieu E., Bouyoucef K., 1994, J. Mod. Opt. 41, 1537
Lannes A., Anterrieu E., Bouyoucef K., 1995, J. Mod. Opt. in press
Lelièvre G., Wlérick G., Sebag J., Bijaoui A., 1994, C. R. Acad. Sci. Paris 318, 905
McMahon R.G., Omont A., Bergeron J., Kreysa E., Haslam C.G.T., 1994, MNRAS 267, L9
Meisenheimer K., Heavens A.F., 1986, Nat 323, 419
Meisenheimer K., Röser H.-J., Schlötelburg M., 1995, A&A in press
Merritt D., Tremblay B., 1993, AJ 106, 2229
Owen F.N., Eilek J., Keel W.C., 1990, ApJ 362, 449
Salter C.J., Chini R., Haslam C.G.T. et al., 1989, A&A 220, 42
Sparks W.B., Laing R.A., Jenkins C.R., 1988, AJ 95, 1684
Steppe H., Salter C.J., Chini R. et al., 1988, A&AS 75, 317
White R.E., Sarazin C.L., 1988, ApJ 335, 688
Young J.S., Xie S., Kenney J.D.P., Rice W.L., 1989, ApJS 70, 699
Zeilinger W.W., Moller P., Stiavelli M., 1993, MNRAS 261, 175

This article was processed by the author using Springer-Verlag LaTeX A&A style file version 3.